The Astrophysical Journal, 671:303–309, 2007 December 10

DYNAMICAL PROPERTIES OF $z \sim 2$ STAR-FORMING GALAXIES AND A UNIVERSAL STAR FORMATION RELATION[1]

N. Bouché,[2] G. Cresci,[2] R. Davies,[2] F. Eisenhauer,[2] N. M. Förster Schreiber,[2] R. Genzel,[2,3] S. Gillessen,[2] M. Lehnert,[2,4] D. Lutz,[2] N. Nesvadba,[2,4] K. L. Shapiro,[5] A. Sternberg,[6] L. J. Tacconi,[2] A. Verma,[7] A. Cimatti,[8] E. Daddi,[9] A. Renzini,[10] D. K. Erb,[11] A. Shapley,[12] and C. C. Steidel[13]

Received 2007 March 21; accepted 2007 July 28

ABSTRACT

We present the first comparison of the dynamical properties of different samples of $z \sim 1.4$–3.4 star-forming galaxies from spatially resolved imaging spectroscopy from SINFONI/VLT integral field spectroscopy and IRAM CO millimeter interferometry. Our samples include 16 rest-frame UV-selected, 16 rest-frame optically selected, and 13 submillimeter galaxies (SMGs). We find that rest-frame UV and optically bright ($K < 20$) $z \sim 2$ star forming galaxies are dynamically similar, and follow the same velocity-size relation as disk galaxies at $z \sim 0$. In the theoretical framework of rotating disks forming from dissipative collapse in dark matter halos, the two samples require a spin parameter $\langle\lambda\rangle$ ranging from 0.06 to 0.2. In contrast, bright SMGs ($S_{850\,\mu\mathrm{m}} \geqslant 5$ mJy) have larger velocity widths and are much more compact. Hence, SMGs have lower angular momenta and higher matter densities than either the UV or optically selected populations. This indicates that dissipative major mergers may dominate the SMGs population, resulting in early spheroids, and that a significant fraction of the UV/optically bright galaxies have evolved less violently, either in a series of minor mergers, or in rapid dissipative collapse from the halo, given that either process may leads to the formation of early disks. These early disks may later evolve into spheroids via disk instabilities or mergers. Because of their small sizes and large densities, SMGs lie at the high surface density end of a universal (out to $z = 2.5$) "Schmidt-Kennicutt" relation between gas surface density and star formation rate surface density. The best-fit relation suggests that the star formation rate per unit area scales as the surface gas density to a power of $\sim$1.7, and that the star formation efficiency increases by a factor of 4 between non-starbursts and strong starbursts.

Subject headings: cosmology: observations — galaxies: evolution — infrared: galaxies

Online material: color figures

1. INTRODUCTION

Deep surveys have become efficient in detecting $z \sim 1.5$–3 star-forming galaxy populations (e.g., Steidel et al. 1996, 2004; Franx et al. 2003; Daddi et al. 2004a; Chapman et al. 2005). Large samples are now available, based on their rest-frame UV magnitude/color properties (the so-called BX/BM criterion; Adelberger et al. 2004; Steidel et al. 2004; Erb et al. 2006a), their rest-frame optical magnitude/color properties ("star forming" or s-BzK criterion; Daddi et al. 2004b, 2004a; Kong et al. 2006; Gemini Deep Deep Survey [GDDS], Abraham et al. 2004), or their submillimeter flux densities (Smail et al. 2002; Chapman et al. 2004, 2005; Pope et al. 2006). The BX/BM or s-BzK selection criteria sample luminous ($L \sim 10^{11}$–$10^{12}\ L_{\odot}$) galaxies with star formation rates $\mathcal{R}_{*} \sim 10$–$300\ M_{\odot}\ \mathrm{yr}^{-1}$, and with ages from 50 Myr to 2 Gyr (Erb et al. 2006b; Daddi et al. 2004b, 2004a). Bright submillimeter continuum selected systems (SMGs) with $S_{850\,\mu\mathrm{m}} > 5$ mJy sample dusty, gas-rich, and very luminous ($\sim 10^{13}\ L_{\odot}$) galaxies with much larger star formation rates $\mathcal{R}_{*} \sim 10^{3}\ M_{\odot}\ \mathrm{yr}^{-1}$ (Blain et al. 2002; Smail et al. 2002; Chapman et al. 2005).

It is obviously desirable to better understand the evolution of these different galaxy populations, as well as their relation to each other. A powerful new tool comes from spatially resolved dynamical studies. Such measurements are now feasible with near-IR integral field spectrographs (IFUs) on 8 m class telescopes, with SINFONI at the ESO/VLT (e.g., Förster Schreiber et al. 2006) and with OSIRIS on Keck (e.g., Wright et al. 2007), and with high-resolution millimeter interferometry in CO rotation lines, for instance with the IRAM Plateau de Bure Interferometer (PdBI: Guilloteau et al. 1992).

In this paper, we present the first comparison of the different $z \sim 2$ galaxy samples (UV, optical, submillimeter) in terms of their structural and dynamical properties, combining the near-IR IFU and millimeter interferometry techniques. Throughout, we use a ΛCDM cosmology with $\Omega_M = 0.3$, $\Omega_{\Lambda} = 0.7$, and $H_0 = 70\ \mathrm{km\ s^{-1}\ Mpc^{-1}}$.

[1] Based on observations at the Very Large Telescope (VLT) of the European Southern Observatory (ESO), Paranal, Chile, under programs GTO 073.B-9018, 074.A-9011, 075.A-0466, 076.A-0527, 077.A-0576, 078.A-0600, and 079.A-0341 and on observations obtained at the IRAM Plateau de Bure Interferometer (PdBI). IRAM is funded by the Centre National de la Recherche Scientifique (France), the Max-Planck Gesellschaft (Germany), and the Instituto Geografico Nacional (Spain).

[2] Max-Planck-Institut für extraterrestrische Physik (MPE), Giessenbachstr.1, 85748 Garching, Germany.

[3] Department of Physics, Le Conte Hall, University of California, Berkeley, CA 94720.

[4] GEPI, Observatoire de Paris-Meudon, Place Jules Janssen, 92195 Meudon Cedex, France.

[5] Department of Astronomy, Campbell Hall, University of California, Berkeley, CA 94720.

[6] School of Physics and Astronomy, Tel Aviv University, Tel Aviv 69978, Israel.

[7] Department of Astrophysics, University of Oxford, Denys Wilkinson Building, Keble Road, Oxford OX1 3RH, UK.

[8] Universita di Bologna, Via Ranzani 1, I-40127 Bologna, Italy.

[9] Laboratoire AIM, CEA/DSM-CNRS, Université Paris Diderot, DAPNIA/SAp, 91191 Gif sur Yvette, France.

[10] Osservatorio Astronomico di Padova, Vicolo dell'Osservatorio 5, Padova, I-35122, Italy.

[11] Harvard-Smithsonian Center for Astrophysics, 60 Garden Street, Cambridge, MA 02138.

[12] Princeton University Observatory, Peyton Hall, Ivy Lane, Princeton, NJ 08544.

[13] California Institute of Technology, MS 105-24, Pasadena, CA 91125.

2. OBSERVATIONS

As part of our spectroscopic imaging survey of high-redshift galaxies in the near-infrared with the SINFONI (SINS) guaranteed time program, we have been studying the kinematic properties of a substantial sample of $z \sim 1.4$–3.2 galaxies selected with rest-frame UV and optical selection techniques and integral field spectroscopy (Förster Schreiber et al. 2006; Genzel et al. 2006).

For the rest-frame UV sample, we observed 17 galaxies drawn from the Hα survey of Erb et al. (2006a), which were selected by their *UGR* colors down to $R < 25.5$. In the literature (Adelberger et al. 2004), these are referred to as "BX" galaxies (in the redshift range 2.0–2.43) and "BM" galaxies (in the redshift range 1.0–1.5). We detect Hα for 15 BX galaxies at $\langle z \rangle = 2.24$ and 1 BM galaxy at $z = 1.4$. In the sole nondetection, the Hα line happened to fall directly on a strong OH sky line, which prevented meaningful observations. Of these galaxies, 14 have already been presented in Förster Schreiber et al. (2006). As described in Förster Schreiber et al. (2006), the SINFONI BX/BM sample appears to be a fair representation of the larger Erb et al. (2006a) Hα sample in terms of source sizes and dynamical masses. Our selection criteria emphasize marginally brighter ($\langle F(\mathrm{H}\alpha) \rangle \sim 10^{-16}$ compared to 6×10^{-17} erg s^{-1} cm^{-2}) and somewhat broader line width ($\langle v_c \rangle \sim 175 \pm 68$ km s^{-1} rms, compared to 140 km s^{-1}) systems than the average galaxy in the larger sample of Erb et al. (2006a).

We also observed 19 optically selected galaxies, 16 of which are detected in Hα and presented for the first time in this paper. The sample consists of 11 $K_s < 20$ galaxies meeting the s-BzK color criterion of Daddi et al. (2004a), taken from the GOODS-S (Daddi et al. 2004b) and Deep 3a (Kong et al. 2006) fields, and 8 galaxies from the Gemini Deep Deep Survey (GDDS; Abraham et al. 2004) with $K_s \leqslant 20.5$ and $I \leqslant 24.5$. Thus, the 19 optically selected galaxies have similar magnitude limits. From the flux-limited samples, actively star-forming galaxies are selected with the s-BzK color criterion for the 11 BzK galaxies, and by requiring the presence of the [O II] emission line and young stellar populations ("100" category in Abraham et al.) for the GDDS galaxies. All s-BzK and 5 of the 8 GDDS galaxies were detected in Hα. For the three GDDS galaxies, the nondetection of Hα is most likely due to a faint line emission and unfavorable wavelengths (close to the bright sky OH emission line). Table 1 summarizes our subsample sizes.

For meaningful comparisons among the samples, we separate them in two redshift bins, $z = 2.0$–2.4 and $z = 1.35$–1.65. The *K*-selected and Hα-detected sample comprises 10 in the redshift range $z = 2.0$–2.4, ($\langle z \rangle = 2.23$), and two from GDDS. Three BzK and three detected GDDS galaxies are at $\langle z \rangle = 1.52$ (see Table 1).

For all but three galaxies, we employed SINFONI (Eisenhauer et al. 2003) in seeing-limited mode ($0.125'' \times 0.25''$ pixels), resulting in FWHM $\sim 0.5''$ resolution (see Förster Schreiber et al. 2006). Three were observed with adaptive optics (as in Genzel et al. 2006) with $0.050'' \times 0.100''$ pixels, resulting in a FWHM of $0.15''$–$0.35''$. The spectral resolution is about 80 and 100 km s^{-1} FWHM in the *K* and *H* bands. respectively. For a description of data-reduction methods, we refer the reader to Schreiber et al. (2004), Abuter et al. (2006), and Förster Schreiber et al. (2006).

We compare our UV/optically selected galaxies with a sample of SMGs observed at the IRAM Plateau de Bure Interferometer (Downes & Solomon 2003; Genzel et al. 2003; Neri et al. 2003; Kneib et al. 2004; Greve et al. 2005; Tacconi et al. 2006). The SMG sample consists of 10 bright ($S_{850\,\mu\mathrm{m}} \geqslant 5$ mJy) SMGs in the $z \sim 2.2$–3.4 range, from the radio-selected sample of Chapman et al. (2004, 2005). We also include three SMGs from the work of Downes & Solomon (2003), Genzel et al. (2003), and Kneib et al. (2004). The median redshift of the 14 SMGs is $\langle z \rangle = 2.49$.

TABLE 1
SUMMARY OF OUR SUBSAMPLE SIZES

Samples	Observed	Detected	$z = 2$–2.5	$z = 1.35$–1.65
BX/BM	17	16	15	1
K20 (GOODS)	5	5	5	0
s-BzK (Deep 3a)	6	6	3	3
GDDS	8	5	2	3
SMG	13	13	13	0
Total	49	45	38	7

NOTE.—The detections refer to Hα for the rest-frame UV and optically selected galaxies and to CO for the SMGs.

3. RESULTS

From the SINFONI data we extracted Hα fluxes, star formation rates, intrinsic half-intensity radii ($R_{1/2}$), and circular velocities (v_c), which give dynamical masses within $R_{1/2}$. Following the same method as described in Förster Schreiber et al. (2006), we used both the source integrated velocity width and the observed velocity gradient (detected in 14 of the 16 BX/BM, and 13 of the 16 s-BzK/GDDS galaxies) to derive two independent estimates of v_c. To do so quantitatively, we analyzed the data in the framework of simple axisymmetric, rotating disk models, taking into account beam smearing and inclination. In the cases where inclination could not be determined from the Hα morphological aspect ratios, we adopted $\sin i = \langle \sin i \rangle = 2/\pi$.

The Hα detection rate and kinematic properties of the s-BzKs and GDDS galaxies appear slightly different. All eight $z \sim 2$ s-BzKs are detected and well resolved in Hα, with large velocity gradients (>100 km s^{-1}). In contrast, only five (of eight) of the GDDS sources, which are mostly at lower redshifts, are detected in Hα. There is a tendency for all GDDS sources and two of the three, $z \sim 1.5$ s-BzKs to be more compact, with small or modest velocity gradients (40–100 km s^{-1}). For the SMGs, the PdBI observations have established a source size or a significant upper limit in ^{12}CO line emission or 1 mm continuum for eight of the galaxies (Tacconi et al. 2006). Only one of these shows a resolved velocity gradient in CO (SMM J02399−0136; Genzel et al. 2003). The other observed SMGs are too compact to detect kinematic structure at the current best resolution of $\sim 0.5''$. With these data in hand, we are now in a position to carry out a first comparison between the various samples in terms of their velocity and size (§ 3.1), matter densities (§ 3.2), and global star formation relations (§ 3.3).

3.1. *Velocity-Size Relation: Kinematic Comparison of the Samples*

Disk galaxies at $z \sim 0$ exhibit a well-known correlation in the velocity-size plane (Courteau 1997). The velocity-size plane is a powerful tool for constraining the angular momentum properties of our galaxies from a theoretical (e.g., Fall & Efstathiou 1980; Mo et al. 1998, hereafter MMW98) or observational point of view (e.g., Courteau 1997; Puech et al. 2007). In the framework of dissipative collapse to centrifugally supported disks of baryonic gas in dark matter halos (White & Rees 1978; MMW98), the disk scale length R_d is given by

$$R_d \propto v_c \lambda (j_d/m_d) H(z)^{-1}, \quad (1)$$

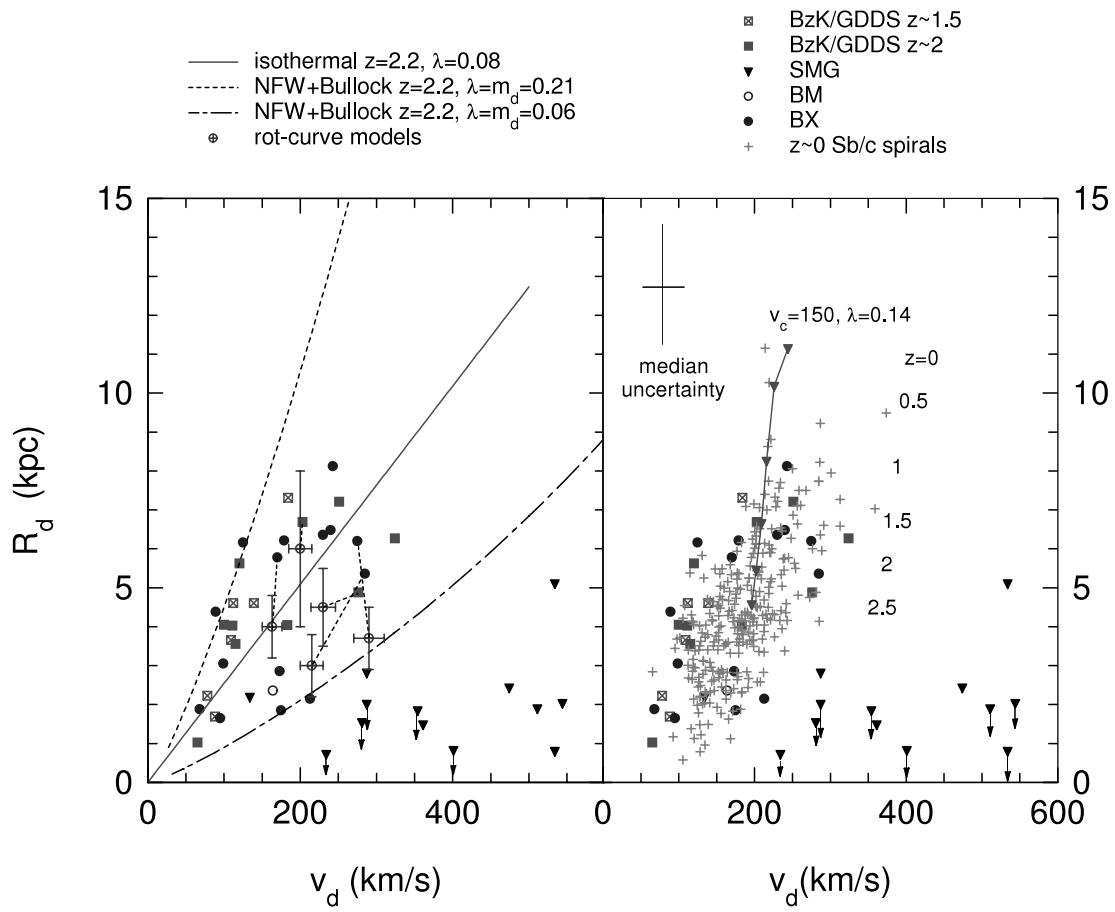

FIG. 1.– *Left*: Exponential disk scale length (R_d) vs. the maximum rotation velocity (V_d) for the different $z \sim 2$ galaxy samples: BX (*filled circles*), BM (*open circles*), SMGs (*filled triangles*), $z \sim 2$ BzK/GDDS (*filled squares*), and $z \sim 1.5$ BzK/GDDS (*open crossed squares*). Whenever possible, an inclination correction was estimated from the intrinsic morphological aspect ratio or assuming $\langle \sin i \rangle = 2/\pi$, as appropriate for a statistical average. For five $z \sim 2$ galaxies we also carried out a full disk modeling, and here we plot the best-fit disk scale length and inclination-corrected maximum disk circular velocity (*crossed open circles*). Heavy dotted lines connect these better estimates with the simpler ones above. The solid line is the best fit to the BX and BzK/GDDS data for an isothermal model of a centrifugally supported disk within a halo of spin parameter of $\lambda = 0.08$. The dash-dotted and dotted curves are MMW98 models for self-gravitating disks in NFW halos for $\lambda = 0.06$ and 0.21, where the disk mass fraction $m_d = \lambda$ (critical disks). *Right*: Comparison of the high-z galaxy sample with the sample of $z \sim 0$ Sb/c disk galaxies of Courteau (1997; *gray crosses*). The solid line with triangles denotes the redshift evolution of a disk from $z = 2.5$ to 0 for a $v_c = 150$ km s^{-1} NFW halo with $\lambda' = m_d = 0.14$ for the halo concentration parameter above. The median uncertainty of the high-z data is indicated at the upper left of the right panel, including fit errors, and also systematic uncertainties in inclination correction and the transformation from observed FWHM sizes to disk scale lengths. Size upper limits are marked as arrows for the SMGs. [*See the electronic edition of the Journal for a color version of this figure*.]

where v_c is the halo circular velocity, λ is the spin parameter of the halo, (j_d/m_d) the ratio of the disk angular momentum fraction, j_d, to the disk to halo mass fraction, m_d, and $H(z)$ is the Hubble parameter at redshift z. The proportionality constant depends on the specific dark matter halo profile and the assumed disk physics. Because $H(z)$ increases by a factor of 3 from $z = 2$ to 0, high-redshift disks ought to be smaller for a given v_c, if the disk spin parameter $\lambda' = \lambda(j_d/m_d)$ does not change with redshift. We assume that the baryons experienced no loss of angular momentum during collapse (Fall & Efstathiou 1980), which implies $j_d/m_d = 1$ and $\lambda' = \lambda$ This condition is supported by our earlier results in Förster Schreiber et al. (2006).

In Figure 1 we show a comparison of the velocity-size properties between our different $z \sim 1.5$–3.4 galaxies (*left panel*) and the $z \sim 0$ Sbc disks from Courteau (1997) (*right panel*). In plotting the high-redshift galaxies, we assume that the exponential disk scale length (R_d) of the Hα emission is equal to the inferred linear, intrinsic half-light radius $R_{1/2}$. This assumption is supported by model disk fits incorporating the beam smearing due to the $\sim$0.5″ FWHM resolution of our data. The maximum circular velocity is determined either from the total velocity width and velocity gradients[14] (when available), or from disk modeling for five of our $z \sim 2$ galaxies. Systematic uncertainties (included in the typical error given as a large cross in the right panel of Fig.1) are substantial, especially in the R_d coordinate, which is strongly affected by the clumpy and often asymmetric Hα brightness distribution.

The immediate question is whether the $z \sim 2$ galaxies truly are rotating disks in gravitational equilibrium. This question can at present be addressed quantitatively only for a subset of about a dozen or so of our BX/s-BzK galaxies for which good quality, two-dimensional kinematics can be extracted (Förster Schreiber et al. 2006; Genzel et al. 2006; G. Cresci et al., in preparation). Within this subset, a rotating disk interpretation is compelling for

[14] Models of rotating disks with appropriate parameters for BzK/BX/BM/GDDS galaxies and observed with $\sim$0.5″ FWHM suggest $v_c \sin i \sim 0.42\Delta v$(FWHM) and $v_c \sin i \sim 0.67 v_r$, where Δv is the total FWHM line width of the galaxy, and v_r is half of the maximum velocity gradient observed on either side of the galaxy (Förster Schreiber et al. 2006).

more than half of the cases (K. Shapiro et al., in preparation), indicating that at least 50% of our sources are indeed disks. There are a few galaxies (at most four) for which a merger interpretation is more appropriate, in which case the velocity-size plot is still useful in a virial sense.

Independent of the modeling details, there are two significant conclusions from Figure 1. First, the BX/BM and s-BzK/GDDS galaxies we have observed have comparable dynamical properties. The BX/BM and s-BzK criteria select largely overlapping populations (at least down to $K_s < 20$), in excellent agreement with Reddy et al. (2005) and Grazian et al. (2007). Second, and in contrast to the rest-frame UV/optically selected galaxies, SMGs occupy a very different part of the v_c-R_d plane. SMGs are more compact and at the same time have greater velocity widths (as in Swinbank et al. 2004) than the UV/optically selected galaxies (by a factor of $\sim$2 in each coordinate; Greve et al. 2005; Tacconi et al. 2006; Iono et al. 2006). SMGs appear to be dynamically distinct from the UV/optically selected samples and appear to have low orbital angular momenta. Since gas-rich major mergers are efficient at removing angular momentum through large-scale gravitational torques (Barnes & Hernquist 1996), it is tempting to conclude that this dichotomy is a result of whether or not a galaxy has recently undergone a major merger. Note that in a gas-rich major merger, the gas settles into a central disk rapidly, in 10^8 yr (Barnes & Hernquist 1996; Iono et al. 2004), justifying a rotating disk approximation used in Figure 1. In fact, even in early stage mergers, such as NGC 6240, the molecular gas is centered between the two radio/near-infrared nuclei (Tacconi et al. 1999; Iono et al. 2007) and is also the center of rotation and marks the maximum of velocity dispersion in both the stars and the gas.

Surprisingly, the right panel of Figure 1 shows that the rest-frame UV/optically selected $z \sim 2$ galaxies also overlap with the velocity-size distribution of the $z \sim 0$ disks of Courteau (1997), as also found from recent IFU results on $z \leqslant 0.6$ star-forming galaxies (Puech et al. 2007). The spread in the v_c-R_d plane is comparable to that of $z \sim 0$ disks. The five $z \sim 2$ galaxies with full two-dimensional modeling confirm that the overlap with the $z \sim 0$ galaxies is not an artifact of our data. The overlap with the $z = 0$ sample suggests that there exists a significant population of $z \sim 2$ galaxies with total angular momenta comparable to $z \sim 0$ disk galaxies. In contrast, our $z \sim 2$ galaxies do not overlap with the distribution of local early type galaxies in this plane (e.g., in a comparison with the data from Bender et al. 1992).

The solid line in the left panel of Figure 1 represents the best-fit halo angular momentum parameter λ (=0.08) to our UV/optically selected galaxies, in the limit of isothermal ($v_c = \text{const}$) dark matter halo profiles in equation (1). The dotted and long-dashed curves in Figure 1 represent models obtained from equation (1) with more realistic NFW (Navarro et al. 1997) dark matter halos, with the inclusion of self-gravity of the disks as prescribed in MMW98, and with the z-scaling of halo concentration parameters found by Bullock et al. (2001): $c_{\rm vir} = 9(M_{\rm vir}/1.1 \times 10^{13}\ M_{\odot})^{-0.13}/(1+z)$.

Such MMW98 models with $\lambda = 0.06$ and $\lambda = 0.21$ bracket our high-z galaxies. The average λ-parameter we deduce is twice the average angular momentum parameter found in dark matter simulations ($\lambda = 0.04$–0.05; e.g., MMW98). Observations of a larger sample are required to test whether this result is an artifact of our selections, or truly an intrinsic property of the high-z star-forming galaxies. In addition, to be so actively star forming, the baryonic disks must be strongly self-gravitating, and may even be unstable under their own gravity, with $m_d \geqslant \lambda$ (MMW98). This implies that the galaxies we are observing have disk mass fractions m_d of $\sim$0.08 on average, corresponding to about half of the cosmic baryon fraction ($\Omega_{\rm baryon}/\Omega_{\rm dark\ matter} \sim 0.18$; Spergel et al. 2007).

3.1.1. *Additional Considerations*

In comparing SMGs with UV/optically selected galaxies, it is important to establish whether Hα on the one hand, and CO/millimeter continuum emission on the other hand, are good tracers of the global distribution of gas and star formation in dusty star-forming galaxies. Since SMGs appear to be "scaled-up" (more luminous and more gas rich) versions of $z \sim 0$ ultraluminous infrared galaxies (ULIRGs; Tacconi et al. 2006), one can gain insights on the SMG properties from the $z \sim 0$ analogs. For the ULIRG population, the answer to the above question is unequivocally positive in terms of the CO/millimeter-continuum emission (cf. Tacconi & Lutz 2001). It is thus very plausible that the millimeter-line and continuum emission trace the distribution of star formation in SMGs as well. Local ULIRGs have small effective radii (inferred from near-IR photometry, tracing the mass), a few kpc or less (Genzel et al. 2003; Tacconi et al. 2001), which are comparable to the CO sizes (Downes & Solomon 1998; Tacconi et al. 1999; Iono et al. 2007). In SMGs CO/millimeter-continuum sizes are also comparable to those in the radio continuum (Tacconi et al. 2006; Chapman et al. 2004), which is likely another good tracer of star formation via the FIR-radio correlation. Thus, the sizes inferred from CO/millimeter-continuum for SMGs are likely representative of the size of the host. In a given SMG, CO/millimeter-continuum emission and Hα emission do not need to originate from the same region(s). SMGs/ULIRGs have the largest dust column densities and extinctions, and thus are the worst cases for Hα observations. UV/optically selected galaxies likely have much lower dust content and extinction than SMGs, and it thus seems safe to assume that Hα is a good tracer of the overall star formation distribution in these sources.

Similarly, it is important to establish, for the SMGs, whether the line widths measured from the CO line emission are representative of the gravitational potential, and whether (AGN-driven) outflows play any significant role. Double-peaked profiles occur when two close nuclei are orbiting each other in a rotating nuclear ring, or disk. Such profiles have been observed in $z \sim 0$ ULIRGs (Narayanan et al. 2005), such as Arp 220, and the majority (50%) of SMGs (Tacconi et al. 2006). In the case when rotation dominates, the two profiles are broad and symmetric. Narayanan et al. (2006) showed that the kinematic signatures of AGN-driven outflows are asymmetric profiles in both the line width of each component and the relative intensity. However, the outflow signature does not dominate the overall kinematics, and may be visible only 25% of the time (Narayanan et al. 2006). Given that in local ULIRGs the signatures of molecular outflows have not been observed, and that the AGN contribution to the SMGs FIR flux is small (see § 3.3), it is extremely unlikely that the molecular line emission in SMGs is affected by molecular outflows.

In their study of a larger sample of $S_{850\ \mu{\rm m}} \geqslant 5$ mJy SMGs with radio detections (from which our SMG sample was drawn to a large extent), Chapman et al. (2005) find that the majority of SMGs with spectroscopic redshifts have rest-frame UV colors compatible with the BX criterion of Steidel et al. (2004). This overlap in color is compatible with the dichotomy we find from our dynamical measurements, for the following reason. The average R-band magnitude of the SMGs in the Chapman et al. (2005) sample is 24.9, or about 1.3 mag fainter than the average R-band magnitude of our BX sources. The BX (or s-BzK)-component of an SMG comes from low-extinction star-forming regions that contribute only a small fraction of the average star

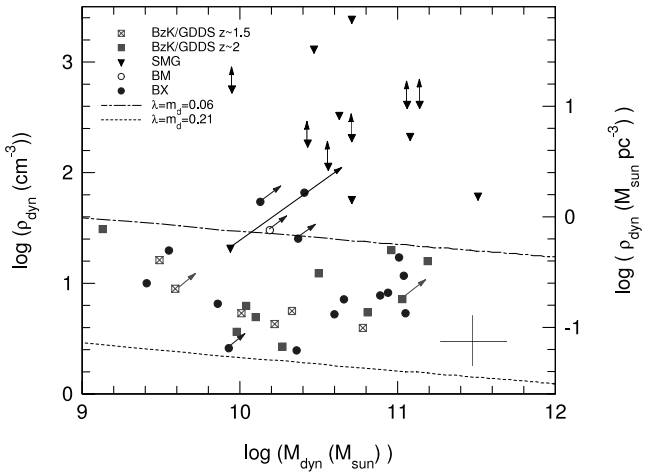

FIG. 2.—Global matter volume density ($\rho_{\rm dyn} = M_{\rm dyn}/[2\pi(R_{1/2})^2 h_z]$), with z-scale height h_z, as a function of dynamical mass within $R_{1/2}$, for the various samples. The dashed and dash-dotted curves are the two bracketing MMW98 models from Fig. 1, and symbols are the same as in Fig. 1. We assumed a ratio of $h_z/R_{1/2} \sim 0.25$, as inferred by Tacconi et al. (2006), Förster Schreiber et al. (2006), Genzel et al. (2006), and Elmegreen & Elmegreen (2006). Size upper limits are marked as vertical arrows. Inclination limits are marked as diagonal arrows. The SMG SMM 14011+0252 is likely at low inclination, and its true location may be significantly to the right (*long arrow*). The SMGs have matter densities (>100 cm^{-3}) similar to those of local ellipticals and spheroids (Kormendy 1989). [*See the electronic edition of the Journal for a color version of this figure.*]

formation rate (less than 10%), similar to local ULIRGs (Tacconi & Lutz 2001). Our dynamical dichotomy between submillimeter and rest-frame optically/UV-selected sources thus is not at odds with the optical/UV photometric properties of the two populations.

3.2. *SMGs are Much Denser than UV/Optically Selected Galaxies*

Figure 2 shows a comparison of the various high-z samples and MMW98 disk models in the dynamical disk mass-volume density plane. As in Figure 1, UV and optically selected galaxies and SMGs are clearly separated, while star-forming BX/BM and s-BzK/GDDS galaxies overlap. To the extent that CO and Hα measurements provide fair and comparable estimates of the dynamical properties of each galaxy, the separation between $z \sim 2$ UV/optically selected galaxies and SMGs is almost all due to their matter density and not due to the mass enclosed within the half-light radius of the CO/Hα data, except for galaxies in the $z \sim 1.5$ subsample, which have smaller dynamical masses. Volume/surface densities of UV/optically selected galaxies are similar to those in $z \sim 0$ disks. SMGs are on average 1–2 orders of magnitude denser, and their average matter densities range from 100 to 1000 cm^{-3}. As we will show in the next section, they also have high surface densities (see also Nesvadba 2007). Such high surface/matter densities are higher than local spheroid densities (Bender et al. 1992) and similar to that of $z \sim 1.5$ spheroids, which are also smaller and denser than local spheroids (Trujillo et al. 2006; Longhetti et al. 2007). The circular velocities (200–500 km s^{-1}) and potential wells of SMGs are similar to $z \sim 0$ spheroids as already found by Tacconi et al. (2006) and Swinbank et al. (2006).

3.3. *A Universal Schmidt-Kennicutt Relation*

In Figure 3, we show the star formation rate surface density [$\Sigma_{\rm sf} = \mathcal{R}_*/(\pi R_{1/2}^2)$] as a function of gas surface density ($\Sigma_{\rm gas}$; *left panel*) and of gas density divided by dynamical time $\tau_{\rm dyn} = R_{1/2}/v_c$ (*right panel*). The star formation rates $\mathcal{R}_*$ for the UV/optically selected galaxies are from our Hα luminosities, corrected for extinction (Erb et al. 2006a, 2006b; Daddi et al. 2004a) and applying $\mathcal{R}_* = L({\rm H}\alpha)/7.4 \times 10^{40}$ erg s^{-1}. The latter relationship is taken from Kennicutt (1998, hereafter K98) with a correction factor of 0.6 to convert the 0.1–100 $M_\odot$ Salpeter initial mass function (IMF) used by K98 to a Chabrier IMF. Star formation rates for the SMGs are from 850 μm flux densities and $\mathcal{R}_* = 110 S_{850\,\mu{\rm m}}$ (mJy), derived from the Pope et al. (2006) average conversion from $S_{850\,\mu{\rm m}}$ to FIR luminosity and a continuous star formation model. SMGs with $S_{850\,\mu{\rm m}} \geqslant 5$ mJy form stars at a rate an order of magnitude greater than the UV/optically selected galaxies, given that recent *Spitzer* IRS spectra of SMGs have shown that the SMGs are indeed powerful starbursts and not X-ray-obscured AGNs (Lutz et al. 2005; Valiante et al. 2007; Pope et al. 2007). The gas surface densities ($\Sigma_{\rm gas}$) are computed using measured gas fractions ($f_{\rm gas}$) from the molecular gas content for the SMGs, and assuming $f_{\rm gas} = 0.4$ for the rest-frame UV and optically selected galaxies, as described below.

Figure 3 shows that there is a fairly tight relationship between $\Sigma_{\rm sf}$ and $\Sigma_{\rm gas}$ (*left*), or $\Sigma_{\rm gas}/\tau_{\rm dyn}$ (*right*). Combining our high-z galaxy data with the local star-forming galaxies (*gray crosses*) in K98, we find that there appears to be a universal Schmidt-Kennicutt relationship, independent of redshift out to $z = 2.5$. The larger star formation rates of SMGs can be understood almost solely as a consequence of their smaller sizes and larger surface densities compared to those of UV/optically selected galaxies.

In constructing Figure 3 we made an important assumption that differs from K98, which changes the resulting correlations quantitatively but not qualitatively. A number of studies during the last decade have yielded compelling evidence that the conversion factor from ^{12}CO line intensity to total molecular hydrogen gas mass drops significantly, and perhaps suddenly, beyond gas surface densities of $\sim 10^2\ M_\odot$ pc^{-2} (Wild et al. 1992; Solomon et al. 1997; Downes & Solomon 1998; Oka et al. 1998; Rosolowsky et al. 2003; Davies et al. 2004; Hinz & Rieke 2006). As a consequence, we took, as in K98, a Galactic conversion factor [$X_G = 2$–3×10^{20} cm^{-2}/(K km s^{-1})] for the normal galaxies in the K98 sample, but adopted $X = 0.25 X_G$ for the starbursts/(U)LIRGs in K98, which is an average of the values obtained in the above references for high gas density/star formation density galaxies. For the high-z galaxies we derived gas surface densities from the dynamical mass densities [$\Sigma_{\rm gas} = f_{\rm gas} M_{\rm dyn}(R \leqslant R_{1/2})/(\pi R_{1/2}^2)$, with $M_{\rm dyn} = v_c^2 R_{1/2}/G$] and assumed a constant gas fraction of 0.4, which is motivated by the gas fraction found in SMGs with the same $X = 0.25 X_G$ (U)LIRG conversion factor (Greve et al. 2005; Tacconi et al. 2006). With a Galactic conversion factor, the gas masses of local ULIRGs and SMGs would exceed their dynamical masses by a factor of 2. The above relations for the X-factor are appropriate for solar metallicity. Theoretical considerations (Maloney & Black 1988; Wall 2007) suggest that the conversion factor from CO flux to gas mass may increase with decreasing metallicity. However, there is no unanimous conclusion from the existing literature whether (Wilson 1995; Arimoto et al. 1996) or not (Rosolowsky et al. 2003) such an effect is seen in the Local Group of galaxies and how large it is. We have therefore assumed the solar metallicity conversion factors throughout.

For the Chabrier (2003) stellar mass function used here, the best-fit power laws to both low- and high-z galaxies yield universal Schmidt-Kennicutt relations of the forms

$$\Sigma_{\rm sf}(M_\odot\ {\rm yr}^{-1}\,{\rm kpc}^{-2}) = 9.3(\pm 2) \times 10^{-5} \left[\Sigma_{\rm gas}(M_\odot {\rm pc}^{-2})\right]^{1.71(\pm 0.05)},$$
$$\Sigma_{\rm sf}(M_\odot\ {\rm yr}^{-1}\,{\rm kpc}^{-2}) = 0.037(\pm 0.004) \times \left[\Sigma_{\rm gas}/\tau_{\rm dyn}(M_\odot\ {\rm yr}^{-1}\ {\rm kpc}^{-2})\right]^{1.14(\pm 0.03)}, \quad (2)$$

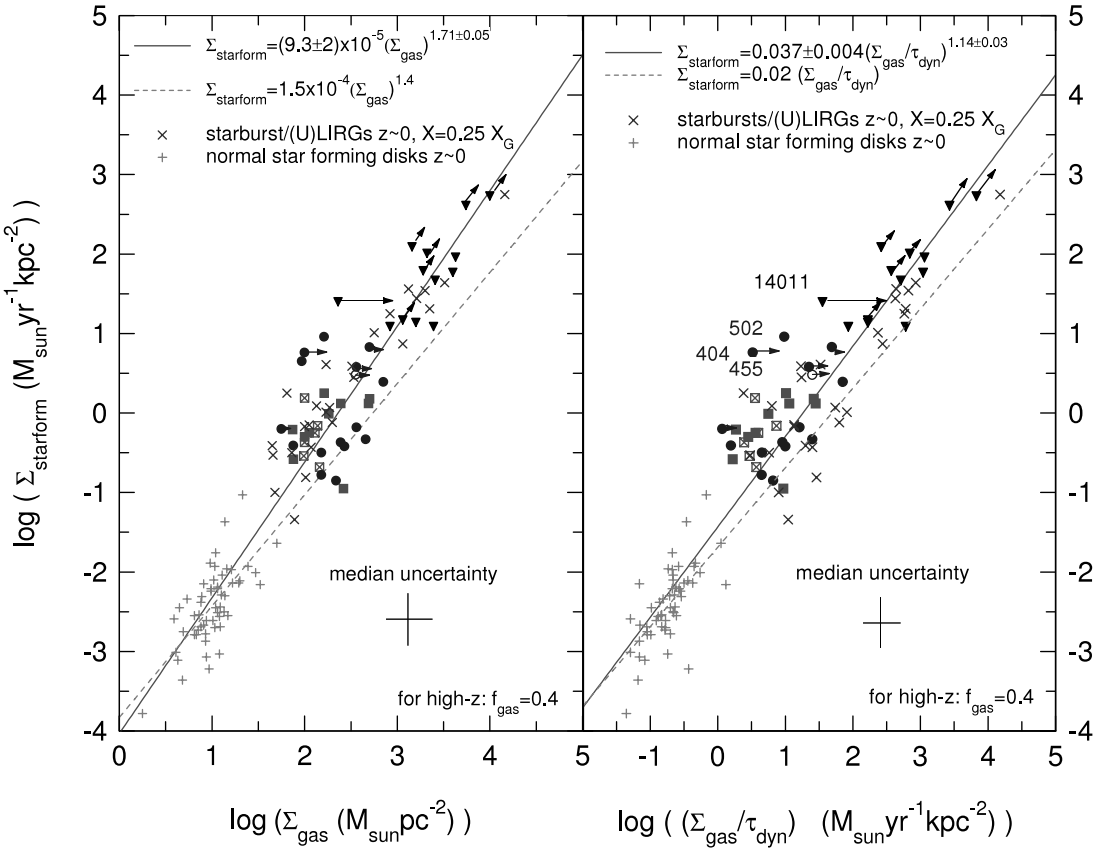

FIG. 3.— Schmidt-Kennicutt relations for low- and high-z galaxies. The symbols for high-z galaxies are the same as in Fig. 1. Gray crosses and stars denote normal galaxies and starbursts/luminous infrared galaxies from Kennicutt (1998; see their Figs. 6 and 7). The median uncertainty of the data points (including uncertainties in inclination correction) is denoted by a large cross. The vertical axis is the star formation rate surface density, $\Sigma_{sf} = \mathcal{R}_*/\pi R_{1/2}^2$, for a Chabrier (2003) stellar mass function. The horizontal axis in the left panel is the gas surface density, and in the right panel the gas surface density divided by dynamical time $\tau_{dyn} = R_{1/2}/v_c$. The solid red curve is the best-fit power law to all low- and high-z data except the outlier SMM 14011+0252 (Nesvadba 2007). The dotted gray curves are the relationships proposed in Kennicutt (1998; $\Sigma_{sf} \sim 0.02\Sigma_{gas}/\tau_{dyn}$ and $\Sigma_{sf} = 1.5\times10^{-4}[\Sigma_{gas}]^{1.4}$), which assume a constant CO-H_2 conversion factor for all galaxies. Of the three prominent BX outliers above the correlation, two (BX 1623−455 and BX 1623−502, denoted in the figure) are found by Erb et al. (2006a) to have a very small ($\leqslant$0.1) ratio of stellar mass to dynamical mass, and thus very likely have gas fractions higher than assumed here. BX 404 and the SMG SMM 14011+0252 are likely at low inclination, and their true location may be significantly to the right. [*See the electronic edition of the Journal for a color version of this figure*.]

where error bars are 1 σ uncertainties to the fit. The power-law index in the first relation is significantly greater than given in K98 ($\Sigma_{sf} \sim \Sigma_{gas}^{1.4\pm0.15}$). It is also marginally greater than the free-fall index of 1.5. This is perhaps suggestive of a collisional or pressure enhancement of the star formation rate at high densities. In contrast to equation (7) of K98 ($\Sigma_{sf} \sim 0.02\Sigma_{gas}/\tau_{dyn}$), the second relationship implies a density-dependent star formation efficiency. Equation (2) implies that $z \sim 2$ SMGs and $z \sim 0$ ULIRGs have a $\sim$4 times greater star formation efficiency than normal galaxies like the Milky Way.

The agreement between low- and high-z Kennicutt-Schmidt laws is remarkable, given our assumption of a constant gas fraction and extinction corrections based on UV/optically data alone. Erb et al. (2006b) have in fact plausibly explained some of the outliers in Figure 3, as these are found to have a very small ($\leqslant$0.1) ratio of stellar mass to dynamical mass and thus likely have gas fractions higher than assumed here.

4. DISCUSSION

From our dynamical comparison (Fig. 1), it appears that rest-frame UV (BX/BM) and optically selected star-forming galaxies (s-BzK) have similar properties, and probably are drawn from overlapping populations down to $K_s < 20$, in agreement with the conclusions reached by Reddy et al. (2005) and Grazian et al. (2007) on the basis of optical/UV photometry.

The most important differences in dynamical/star-forming properties between UV/optical star-forming galaxies and SMGs are the smaller sizes (Fig. 1) and much larger surface/volume densities of the SMGs (Fig. 2). This strong dichotomy may depend on whether or not a galaxy has recently undergone a major merger, resulting in a large loss of angular momentum, and whether the resulting remnant has been transformed into a dense, spheroidal component. This scenario is supported by the comparison of the SMG properties to those of spheroids, and by recent high-resolution millimeter interferometry, which shows that several of the SMGs in Figure 1 could be major mergers (Tacconi et al. 2006, and in preparation), as suspected for some time (Smail et al. 2002) and from morphological studies (Conselice et al. 2003).

Given that the kinematics of UV and optical star-forming galaxies are consistent with that of large protodisks, these systems may have evolved in a less violent fashion through a series of minor mergers, or through cold gas flows from the halo (Keres et al. 2005; Dekel & Birnboim 2006). In the simplest evolutionary model of dissipative accretion, disk scale lengths would be expected to increase by a factor of $1/H(z)$, or 3 between $z = 2$ and $z = 0$ in a ΛCDM cosmology. Taking into account the much smaller concentration parameters at high z suggested by the Bullock et al. (2001), scaling this growth factor would be smaller but would still push the larger, more massive $z \sim 2$ disks way above the location of most $z \sim 0$ disks (right panel of Fig.1). A still smaller

growth factor would be predicted if the baryonic disk mass fraction increases with decreasing redshift (Somerville et al. 2006). Alternatively, and perhaps more likely, some fraction of the $z \sim 2$ disks we are observing may have been subsequently destroyed and converted to spheroids by mergers or secular evolution (van den Bosch 2002; Immeli et al. 2004; Förster Schreiber et al. 2006; Genzel et al. 2006, Governato et al. 2006), in agreement with the cosmic volume density of BX/s-BzK and their clustering (Adelberger et al. 2004, 2005; Kong et al. 2006). Substantial further growth of the disks may also have been inhibited by large negative feedback from AGN/star formation (van den Bosch 2002), or by shock quenching when the halos exceeded a mass of a few $10^{12}\,M_{\odot}$ (Dekel & Birnboim 2006; Birboim et al. 2007). Future dynamical studies with higher spatial resolution will explore the redshift range $z \sim 1.5$ further to test whether the possible trend in the UV/optically selected galaxies for smaller sizes and circular velocities at $z \sim 1.5$ (relative to $\sim$2.3) is a consequence of this evolutionary scenario.

Given that SMGs with $S_{850\,\mu\mathrm{m}} \geqslant 5$ mJy have small sizes and large matter densities, they lie at the high surface density end of a universal (out to $z = 2.5$) Schmidt-Kennicutt relation (Fig. 3). Since the Schmidt-Kennicutt relation implies that the star formation rate per gas particle increases with gas surface density, SMGs must naturally be more luminous than their UV/optically selected kin and form stars at a rate an order of magnitude greater than the UV/optically selected galaxies, despite similar dynamical masses.

We are grateful to the staff of Paranal Observatory for their support, and the SINFONI team for their hard work on the instrument that has made this research possible. We also thank the SMG team, A. Blain, F. Bertoldi, S. Chapman, P. Cox, T. Greve, R. Ivison, R. Neri, A. Omont, and I. Smail. We acknowledge useful discussions with A. Burkert, A. Dekel, T. Naab, and E. Quataert. N. M. F. S. acknowledges support by the Priority Programme 1177 of the Deutsche Forschungsgemeinschatt. We thank the anonymous referee for his/her critical comments that led to an improved manuscript.

REFERENCES

Abraham, R. G., et al. 2004, AJ, 127, 2455
Abuter, R., Schreiber, J., Eisenhauer, F., Ott, T., Horrobin, M., & Gillesen, S. 2006, NewA, 50, 398
Adelberger, K. L., Steidel, C. C., Pettini, M., Shapley, A. E., Reddy, N. A., & Erb, D. K. 2005, ApJ, 619, 697
Adelberger, K. L., Steidel, C. C., Shapley, A. E., Hunt, M. P., Erb, D. K., Reddy, N. A., & Pettini, M. 2004, ApJ, 607, 226
Arimoto, N., Sofue, Y., & Tsujimoto, T. 1996, PASJ, 48, 275
Barnes, J. E., & Hernquist, L. 1996, ApJ, 471, 115
Bender, R., Burstein, D., & Faber, S. M. 1992, ApJ, 399, 462
Birnboim, Y., Dekel, A., & Neistein, E. 2007, MNRAS, 380, 339
Blain, A. W., Smail, I., Ivison, R. J., Kneib, J.-P., & Frayer, D. T. 2002, Phys. Rep., 369, 111
Bullock, J. S., Kolatt, T. S., Sigad, Y., Somerville, R. S., Kravtsov, A. V., Klypin, A. A., Primack, J. R., & Dekel, A. 2001, MNRAS, 321, 559
Chabrier, G. 2003, PASP, 115, 763
Chapman, S. C., Blain, A. W., Smail, I., & Ivison, R. J. 2005, ApJ, 622, 772
Chapman, S. C., Smail, I., Windhorst, R., Muxlow, T., & Ivison, R. J. 2004, ApJ, 611, 732
Conselice, C. J., Chapman, S. C, Windhorst, R. A. 2003, ApJ, 596, 5L
Courteau, S. 1997, AJ, 114, 2402
Daddi, E., Cimatti, A., Renzini, A., Fontana, A., Mignoli, M., Pozetti, L., Tozzi, P., & Zamorani, G. 2004a, ApJ, 617, 746
Daddi, E., et al. 2004b, ApJ, 600, L127
Davies, R., Tacconi, L. J., & Genzel, R. 2004, ApJ, 602, 148
Dekel, A., & Birnboim, Y. 2006, MNRAS, 368, 2
Downes, D., & Solomon, P. 1998, ApJ, 507, 615
———. 2003, ApJ, 582, 37
Eisenhauer, F., et al. 2003, Proc. SPIE, 4841, 1548
Elmegreen, B. G., & Elmegreen, D. M. 2006, ApJ, 650, 644
Erb, D. K., Steidel, C. C., Shapley, A. E., Pettini, M., Reddy, N. A., & Adelberger, K. L. 2006a, ApJ, 646, 107
———. 2006b, ApJ, 647, 128
Fall, S. M., & Efstathiou, G. 1980, MNRAS, 193, 189
Förster Schreiber, N. M., et al. 2006, ApJ, 645, 1062
Franx, M., et al. 2003, ApJ, 587, L79
Genzel, R., et al. 2006, Nature, 442, 786
Genzel, R., Baker, A. J., Tacconi, L. J., Lutz, D., Cox, P., Guilloteau, S., & Omont, A. 2003, ApJ, 584, 633
Governato, F., Willman, B., Mayer, L., Brooks, A., Stinson, G., Valenzuela. O., Wadsley. J & Quinn, T. 2007, MNRAS, 374, 1479
Grazian, A., et al. 2007, A&A, 465, 393
Greve, T. R., et al. 2005, MNRAS, 359, 1165
Guilloteau, S., et al. 1992, A&A, 262, 624
Hinz, J. L., & Rieke, G. H. 2006, ApJ, 646, 872
Immeli, A., Samland, M., Gerhard, O., & Westera, P. 2004, A&A, 413, 547
Iono, D., Yun, M. S., & Mihos, J. C. 2004, ApJ, 616, 199
Iono, D., et al. 2006, ApJ, 640, L1
———. 2007, ApJ, 659, 283
Kennicutt, R. C., Jr. 1998, ApJ, 498, 541
Keres, D., Katz, N., Weinberg, D. H., & Davé, R. 2005, MNRAS, 363, 2
Kneib, J.-P., van der Werf, P. P., Kraiberg Knudsen, K., Smail, I., Blain, A., Frayer, D., Barnard, V., & Ivison, R. 2004, MNRAS, 349, 1211
Kong, X., et al. 2006, ApJ, 638, 72
Kormendy, J. 1989, ApJ, 342, L63
Longhetti, M., et al. 2007, MNRAS, 374, 614
Lutz, D., Valiante, E., Sturm, E., Genzel, R., Tacconi, L. J., Lehnert, M. D., Sternberg, A., & Baker, A. J. 2005, ApJ, 625, L83
Maloney, P., & Black, J. H. 1988, ApJ, 325, 389
Mo, H. J., Mao, S., & White, S. D. M. 1998, MNRAS, 295, 319 (MMW98)
Narayanan, D., Groppi, C. E., Kulesa, C. A, & Walker, C.K 2005, ApJ, 630, 269
Narayanan, D., et al. 2006, ApJ, 642, L107
Navarro, J. F., Frenk, C. S., & White, S. D. M. 1997, ApJ, 490, 493
Neri, R., et al. 2003, ApJ, 597, L113
Nesvadba, N. 2007, ApJ, 657, 725
Oka, T., Hasegawa, T., Hayashi, M., Handa, T., & Sakamoto, S. 1998, ApJ, 493, 730
Pope, A., Chary, R.-R., Dickinson, M., & Scott, D. 2007, preprint (astro-ph/0612105)
Pope, A., et al. 2006, MNRAS, 370, 1185
Puech, M., Hammer, F., Lehnert, M. D., & Flores, H. 2007, A&A, 466, 83
Reddy, N. A., Erb, D. K.,Steidel, C. C., Shapley, A. E., Adelberger, K. L., & Pettini, M. 2005, ApJ, 633, 748
Rosolowsky, E., Engargiola, G., Plambeck, R. L., & Blitz, L. 2003, ApJ, 599, 258
Schreiber, J., Thatte, N., Eisenhauer, F., Tecza, M., Abuter, R., & Horrobin, M. 2004, in ASP Conf. Ser. 314, Astronomical Data Analysis Software and Systems XIII, ed. F. Ochsenbein, M. G. Allen, & D. Egret (San Francisco: ASP), 380
Smail, I., Ivison, R. J., Blain, A. W., & Kneib, J.-P. 2002, MNRAS, 331, 495
Solomon, P. M., Downes, D., Radford, S. J. B., & Barrett, J. W. 1997, ApJ, 478, 144
Somerville, R. S., et al. 2006, ApJ, submitted (astro-ph/0612428)
Spergel, D., et al. 2007, ApJS, 170, 377
Steidel, C. C., Giavalisco, M., Pettini, M., Dickinson, M., & Adelberger, K. L. 1996, ApJ, 462, L17
Steidel, C. C., Shapley, A. E., Pettini, M., Adelberger, K. L., Erb, D. K., Reddy, N. A., & Hunt, M. P. 2004, ApJ, 604, 534
Swinbank, A. M., Chapman, S. C., Smail, I., Lindner, C., Borys, C., Blain, A. W., Ivison, R. J., & Lewis, G. F.. 2006, MNRAS, 371, 465
Swinbank, A. M., Smail, I. S., Chapman, S. C., Blain, A. W., Ivison, R. J., & Keel, W. C. 2004, ApJ, 617, 64
Tacconi, L. J., Genzel, R., Tecza, M., Gallimore, J. F., Downes, D., & Scoville, N. Z. 1999, ApJ, 524, 732
Tacconi, L. J., & Lutz, D. 2001, Starburst Galaxies (Berlin: Springer)
Tacconi, L. J., et al. 2006, ApJ, 640, 228
Trujillo, I., et al. 2006, MNRAS, 373, 36
Valiante, E., Lutz, D., Sturm, E., Genzel, R.., Tacconi, L. J., Lehnert, M. D., & Baker, A. J. 2007, ApJ, 660, 1060
van den Bosch, F. C. 2002, MNRAS, 332, 456
Wall, W. F. 2007, MNRAS, 379, 674
White, S. D. M., & Rees, M. J. 1978, MNRAS, 183, 341
Wild, W., Harris, A. I., Eckart, A., Genzel, R., Graf, U. U., Jackson, J. M., Russell, A. P. G., & Stutzki, J. 1992, A&A, 265, 447
Wilson, C. D. 1995, ApJ, 448, L97
Wright, S. C., et al. 2007, ApJ, 658, 78